Chalcogenide Letters Vol. 14, No. 12, December 2017, p. 545 - 550

CHARACTERIZATION OF THE Au/ZnSe/In/ZnSe/C (ZIZ) BACK TO BACK SCHOTTKY BARRIERS

S. E. AL GARNI[a *]
[a]*Physics Department, Faculty of Science- Al Faisaliah, King Abdulaziz University, Jeddah- Saudi Arabia*

In this article, we report the design and performance of the ZnSe thin films sandwiched with 75 nm thick slab of indium as promising device for microwave resonating applications. The device is studied by X-ray diffraction, temperature dependent resistivity measurements and impedance spectroscopy in the frequency domain of 0.1-1.8 GHz. The X-ray analysis revealed a metal induced improvement in the crystallization process of the cubic phase of ZnSe. It is also observed that the nanosandwiching of the indium between two layers of ZnSe, significantly lowered the electrical resistivity by 17 times and improved the performance of the ZIZ when used as back to back Schottky device between an Au and carbon electrodes. The impedance spectroscopy analysis has shown that the resistance spectral variation controls the frequency domains of the device. The maximum cutoff frequency was achieved at 4.44 GHz when an input signal of biasing voltage of 0.1 V is dominated with frequency of 1.50 GHz. When the device was tested as microwave resonator it show band stop filter features of notch frequency of 1.0 GHz.

(Received October 15, 2017; Accepted December 13, 2017)

Keyword: ZnSe; nanosandwiching; mechanical; optical gap

1. Introduction

II-VI compound semiconductors have significant applications in optoelectronics. One of these compounds is the ZnSe which is used to form II-VI light-emitting diodes and diode laser. Zinc selenide is the potential candidate for fabrication of laser diode in blue region, besides group III nitrides [1]. ZnSe doped with chromium (ZnSe:Cr) has been used as an infrared laser gain medium emitting at about 2.4 µm [2]. With its optoelectronic characteristics, ZnSe showed good photoresponse, suitable for photosensing and solar cell production [2- 4]. Antohe, S., et al, reported that ZnSe thin films are good candidates that can replace the conventional CdS thin films when used as n-type window layers for solar cells and other optoelectronic devices [5].

Beside these applications, the ZnSe was found to be beneficial for use in thin film transistor technology. When the ZnSe was sandwiched between two layers of InSe it show microwave trapping features with notch frequency of ~ 1100 MHz [6]. The work was motivating for trying to obtain wave trap characteristics using the ZnSe thin layers nanosandwiched with indium. For this reason, here in this work, we will report the effect of an indium layer of 75 nm thick on the structural and electrical properties of ZnSe. In addition to that a back to back Schottky device that use the ZnSe/In/ZnSe as semiconducting layer will be reported and characterized.

2. Experimental details

The ZnSe thin films were grown onto ultrasonically cleaned glass substrates under pressure of 10^{-5} mbar in a VCM 600 vacuum deposition system. The ZnSe thin films were used as substrate to grow 75 nm thick high purity indium. The resulting films were used as substrates to grow another layer of ZnSe to form the ZnSe/In/ZnSe (ZIZ) nanosandwiched structure. The

[*] Corresponding author: seef73@gmail.com

thicknesses were controlled by in situ thickness monitor connected to the quartz crystal inside the vacuum chamber. The X-ray diffraction patterns were recorded using powder diffractometer equipped with Cu Kα radiation Miniflex 600 X-ray unit. The impedance spectra were recorded using an Agilent impedance analyzer. The electrical resistivity was measured using closed cycle cryogenic cryostat attached to a Keithley I-V characterization system.

3. Results and discussion

In this work, we employ the nanosandwiching technique to lower the resistivity of the ZnSe thin films to make it more appropriate for technological applications. In this procedure we have nanosandwiched a layer of thickness of 75 nm between two layers of ZnSe each having thickness of 1.0 μm. The percentage of the indium in the volume of the samples is 3.75%. Because the lattice constants of tetragonal indium are a=4.58 and c=4.86 Å (PDF Card No.: 00-001-1042) [7] with the main reflection plane being best oriented in the (111) direction it was expected to directionally align well with the planes of cubic ZnSe (a=5.667 Å) [8] which are also oriented in the (111) direction. The lattice mismatches between the indium and ZnSe layers are ($\Delta\% = (a_{ZnSe} - a_{In})/a_{ZnSe}$) are 19% and 14% along the a and $c - axes$, respectively. The other features which make the indium preferable for the reduction of the resistance is its work function being 4.12 eV [7] which is very close to that of ZnSe (4.09 eV [9]). Although, the lattice mismatches are very high, for the proposed nanosandwiched samples, the critical thicknesses ($t_c = a_{In}^2/(2|a_{In} - a_{ZnSe}|)$ that allow the growth of interfaces with low level of defect distribution are 10 and 15 nm along the a and $c - axes$, respectively. For this reason a sufficiently thick but still transparent layer of thickness of 75 nm indium was selected.

The geometry of the proposed design is shown in the inset of Fig. 1. The figure also represents the results of the X-ray diffraction patterns for the ZnSe/In(75 nm)/ZnSe (ZIZ) stacked layers being deposited onto glass and gold thin film substrates. The data which was indexed with the help of "TREOR 92" software package is found to exhibit main reflection peak which refers to the cubic ZnSe being oriented in the (111) direction. The result is consistent with the proposed idea before the stacked layers deposition. The ZIZ samples which are deposited onto glass substrates contained only two reflection peaks. The strong one refer to cubic and the weak one refer to hexagonal ZnSe. The hexagonal planes are oriented in the (100) direction. As also seen from the figure, the replacement of glass with Au is associated with the appearance of more peaks that refer to the cubic phase of ZnSe. The Au highly induced the growth of the cubic phase and reduced the hexagonal phase. The ratio of the sum of the intensities of the X-ray that relate to the hexagonal phase to that of cubic one is 34% and 23% for the ZIZ deposited onto glass and Au film, respectively. The lattice constant of the Au is 4.08 ^{o}A. This value lead to a lattice mismatch of 28% between the Au substrate and the ZnSe film. Even though the lattice mismatch is very high, the Au induced the better crystallization of ZnSe. The effectiveness of the Au in improving the crystallization of the ZnSe may be assigned to the bonding mechanism between Au and Se compared to the Zn-Se. The bond length of Au-Se is ~ 2.38 ^{o}A [11] is shorter than that of Zn-Se which is reported to be 2.54 ^{o}A [12]. The Se-Zn-Se bonding angle is 108.2^{o} while that of the Au-Se is ~ 77^{o} (for Au_2Se_2 molecule) [11].

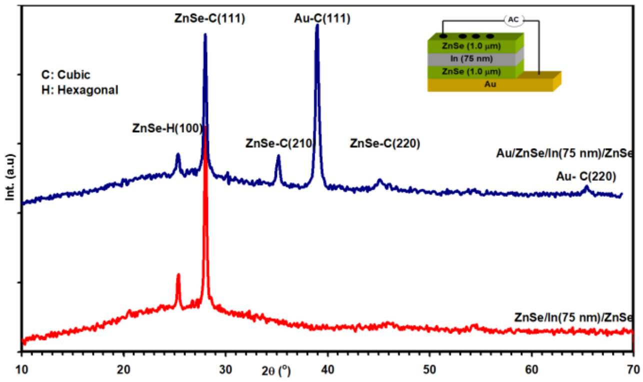

Fig. 1. The X-ray diffraction patterns for the ZnSe/In/ZnSe (ZIZ) and Au/ZnSe/In/ZnSe (Au/ZIZ) films. The inset shows the geometrical presentation of the back to back Schottky device.

The results of the electrical resistivity measurements which were obtained for the ZIZ samples using Hall bar geometry are presented in Fig. 2 (a). The room temperature value of electrical resistivity for the ZnSe sandwiched with 75 nm indium is found to be 1.1 Ωcm. This value is much less than the one reported as 17 Ωcm for the ZnSe thin film [8]. The reduction of the electrical resistivity of ZnSe which was one of the targets of this work may be assigned to the free carrier contribution that arises from the indium nanosandwiching. The hot probe tests has shown that the ZIZ samples exhibit $n-$type conductivity. As the Arrhenius plot of the electrical resistivity which is shown in Fig. 2 (a), reveal very shallow impurity (donor) level of ~8 meV (above 260 K) and 4.0 meV (below 260 K) below the conduction band of ZnSe, the ZIZ is almost of degenerate semiconductor characteristics. The earlier studies that consider the donor levels formation in ZnSe have shown that the Li and Na doping into ZnSe forms a donor level of 15 and 16 meV, respectively [8]. The In, Ga, F and Cl doping forms donor levels at~ 26- 29 meV below the conduction band [8]. It is clear from our work and the published data that the elemental doping forms shallow donor levels in ZnSe.

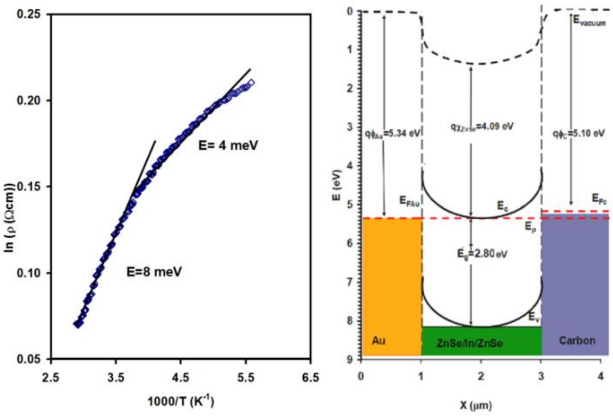

Fig. 2. The electrical resistivity variation with temperature for the ZIZ samples. (b) The energy band diagram for the Au/ZIZ/C back to back Schottky devices.

In order to find application for the ZIZ films, the samples which were deposited onto Au substrates were contacted with carbon point contacts of area of 1.0×10^{-2} cm^{-2}. The carbon was selected owing to its stronger bonding properties. The distance between the electrodes of the device is 2.075 μm. For this electronic structure, the energy band diagram which is designed and shown in Fig. 2 (b) suggest the formation of a back to back Schottky device (BBSD). As the gold work function is 5.34 eV [7] and the electron affinity $(q\chi)$ of ZnSe is 4.09 eV, the Au/ZIZ device form a Schottky contact of barrier height ($q\varphi_{Au/ZIZ} = q\chi - q\phi_{Au}$) of 1.25 eV. On the other side of the sample, with the carbon work function of 5.10 eV [13], the barrier height turnout to be 1.01 eV. The basic idea of this construction is that when one of the devices is forward biased the other is reverse biased. In this operation mode while one of the devices exhibit a widening depletion region, the other one is narrowing. It also allow the "reach through" condition in which the flat bands are formed. This condition is of importance for microwave application of the Schottky diodes. The forward bias cutoff frequency which is given by $f_{co} = (2\pi R_F C_F)^{-1}$ with R_F and C_F being the differential resistance and capacitance, respectively, in a forward bias range of 0.10 to the flat band condition [14]. The value of f_{co} should be lower than its value at zero bias to represent the lower limit for practical applications. The reduction of the series resistance via In sharing is of great importance as it increases the cutoff frequency by at least 17 times (resistivity is reduced 17 times by In nanosandwiching).

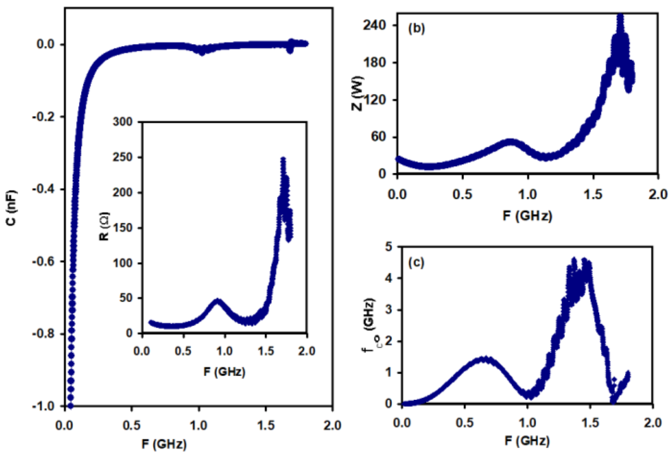

Fig. 3. (a) The capacitance, (b) impedance and (c) cutoff frequency spectra for the Au/ZIZ/C back to back Schottky devices. The inset of (a) show the resistance spectra.

To verify that the ZIZ design improved the performance of ZnSe, the BBSD device was inserted between the terminals of an impedance analyzer that work in the domain range of 0.1-1.8 GHz. The biasing voltage was ~0.10 V. The resulting resistance, capacitance and impedance spectra are shown in Fig. 3. It is clear that both of the resistance (inset of Fig. 3 (a)) and the impedance (Fig. 3 (b)) both exhibit two peaks at 0.95 and 1.71 GHz in the low (below 1.50 GHz) and high (above 1.50 GHz) resistance regions, respectively. The impedance of the device is guided by the resistive part of the BBSD device. On the other hand, the capacitance spectra exhibit negative values with two minima at 1.0 and 1.69 GHz. The negative capacitance effect could be due to surface charge flowing from the ZIZ to the Au or carbon metals. The connection allows flowing of minority carriers to one of the Schottky devices while the other side is forward biased (subjected to majority carrier flow). In addition, the presence of the carbon point's contact as defective contact could be another reason [15]. The surface of the ZIZ is also defective as it is designed to have thickness much larger than the critical thickness. The X-ray analysis of the main peaks using the standard methods [16] reveals a defect density of 2.2× $10^{11} cm^{-2}$ for the ZIZ an Au/ZIZ samples. Even though this value is low compared to defective surfaces ($\delta > 10^{13}\ cm^{-2}$) it is still able to cause the negative capacitance effect. The value of the cutoff frequency as function of incident signals frequency is shown in Fig. 3 (c). Two maximum points of cutoff frequency appeared at 1.38 and 4.44 GHz are observed for an applied signal frequency of 0.67 and 1.49 GHz, respectively. These two f_{co} values represent the high speed capability points with gain value of unity. It is also regarded as the frequency at which the small-signal input gate current is equal to the drain current when the device is used as transistor [14].

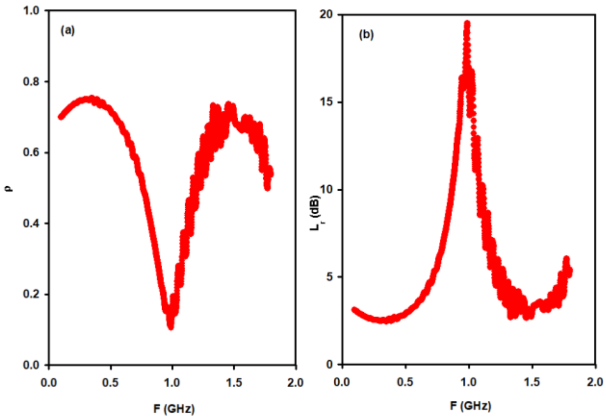

Fig. 4 The reflection coefficient and the return loss spectra for the Au/ZIZ/C back to back Schottky devices

Fig. 4 (a) and (b) show the variation of the magnitude of the reflection coefficient (ρ) and the return loss ($L_r = 20\log(\frac{1}{\rho})$) values as function of incident signal frequency being calculated with the early described procedures [6]. The dynamics of the ρ and L_r spectra reflect the features of band stop filters withy notch frequency of ~1.0 GHz. For all signal frequencies less that one gigahertz, the device behaves as low pass filter, while for greater values it behave as high pass filters [6, 14]. The value of the return loss reaches ~20 at 1.0 GHz indicating the ability of using the Au/ZIZ/C filters as band stop filter at 1.0 GHz. It can also be used as low pass filters beyond this value. Such features of the ZIZ device make it attractive for microwave application.

4. Conclusions

In the current work we have shown the possibility of employing the ZnSe as microwave cavities to oscillate waves of gigahertz frequencies. This property of the device was achieved by the nanosandwiching of a layer of 75 nm thick indium between two layers of ZnSe. In general the ZnSe crystallizes in cubic as major phase associated with hexagonal minor phase. The deposition of the ZnSe onto gold substrates makes the major phase growth more preferable. In addition, an abrupt reduction in the electrical resistivity associated with shallow donor levels was observed upon indium nanosandwichng. The study suggests method to alter the cutoff frequency of microwave devices.

Acknowledgments

This project was funded by the Deanship of Scientific Research (DSR), at King Abdulaziz University, Jaddah, under the grant number G-96-363-38. The authors, therefore, acknowledge with thanks the DSR technical and financial support.

References

[1] M. G. Mahesha, Meghana N. Rashmitha, Meghavarsha Padiyar. Physica B: Condensed Matter (2017).
[2] H. K. Sadekar, Anil Vithal Ghule, and Ramphal Sharma. Composites Part B: Engineering **44(**1), 553 (2013).
[3] A. Rumberg, A., et al. Thin Solid Films **361,** 172 (2000).
[4] S. Antohe, L. Ion, Mihaela Girtan, O. Toma, Romanian Reports in Physics

65(3), 805 (2013).
[5] P. Agarwal, International Journal of Innovative Research and Development **1**(7), 104 (2012).
[6] S. E. Al Garni, Atef F. Qasrawi, IEEE Transactions on Electron Devices **64**(1), 244 (2017).
[7] N. M. Khusayfan, A. F. Qasrawi, Hazem K. Khanfar. Materials Science in Semiconductor Processing **64,** 63 (2017).
[8] O. Madelung, Semiconductors: data handbook. Springer Science & Business Media, 2012.
[9] H. H. Güllü, Ö. Bayraklı, D. E. Yildiz, M. Parlak. Journal of Materials Science: Materials in Electronics **28**, 17806 (2017).
[10] S. G. Kwon, Galyna Krylova, Patrick J. Phillips, Robert F. Klie, Soma Chattopadhyay, Tomohiro Shibata, Emilio E. Bunel et al. Nature materials **14**(2), 215 (2015).
[11] L. Prokeš, Pavel Kubáček, Eladia Maria Peña Méndez, Filippo Amato, José Elias Conde, Milan Alberti, Josef Havel. Chemistry-A European Journal **22**(32), 11261 (2016).
[12] J. Zhou, Yang Li, Xiaohong Wu, Wei Qin. ChemPhysChem **17**(13), 1993 (2016).
[13] A. F. Qasrawi, T. S. Kayed, and Khaled A. Elsayed. Physica E: Low-dimensional Systems and Nanostructures **86,** 124 (2017).
[14] S. M. Sze, Ng, K.K., 2006. Physics of semiconductor devices. John wiley & sons.
[15] X. Wu, E. S. Yang, H. L. Evans, Journal of Applied Physics **68**(6), 2845 (1990).
[16] P. KR Kalita, B. K. Sarma, H. L. Das, Bulletin of Materials Science **23(**4), 313 (2000).